# All-Optical Stern-Gerlach Effect

Aviv Karnieli
*Raymond and Beverly Sackler School of Physics and Astronomy, Tel Aviv University, Ramat Aviv 69978, Tel Aviv, Israel*

Ady Arie
*School of Electrical Engineering, Iby and Aladar Fleischman Faculty of Engineering, Tel Aviv University, Ramat Aviv 69978, Tel Aviv, Israel*

(Received 1 October 2017; published 29 January 2018)

We introduce a novel formalism in which the paraxial coupled wave equations of the nonlinear optical sum-frequency generation process are shown to be equivalent to the Pauli equation describing the dynamics of a spin-1/2 particle in a spatially varying magnetic field. This interpretation gives rise to a new classical state of paraxial light, described by a mutual beam comprising of two frequencies. As a straightforward application, we propose the existence of an all-optical Stern-Gerlach effect, where an idler beam is deflected by a gradient in the nonlinear coupling, into two mutual beams of the idler and signal waves (equivalent to oppositely oriented spinors), propagating in two discrete directions. The Stern-Gerlach deflection angle and the intensity pattern in the far field are then obtained analytically, in terms of the parameters of the original optical system, laying the grounds for future experimental realizations.

DOI: 10.1103/PhysRevLett.120.053901

The Stern-Gerlach (SG) experiment [1–3] is one of the cornerstones of quantum mechanics (QM), providing evidence for the quantum nature of the spin angular momentum. Modern research has given rise to a variety of experimental realizations and proposals of physical systems which exhibit effects analogous to the SG effect [4–7]. Some of these analogies have also emerged in the field of optics: optical fields in a resonant atomic gas have been demonstrated to deflect under the action of an external inhomogeneous magnetic field [8–10]. These analogies, apart from being aesthetically pleasing, may contribute to the fundamental understanding of such physical systems, as well as lead to novel applications.

In the present Letter, we propose the existence of an all-optical SG effect. We demonstrate how the paraxial coupled-wave equations (CWEs) of the sum-frequency generation (SFG) process in nonlinear $\chi^{(2)}$ materials is analogous to the transverse Pauli equation, describing the motion of a non-relativistic spin-1/2 particle in a transverse magnetic field. We show that the nonlinear coupling and the phase-mismatch parameter constitute an effective magnetic field, interacting with a mutual beam comprising a superpoistion of the idler and signal frequencies, the equivalent of a spinor. Consequently, it is shown that a gradient in the nonlinear coupling deflects opposite mutual beams into two discrete angles. The control of light by light in nonlinear $\chi^{(2)}$ media and its applications have been thoroughly established in the past few decades [11]. Along with the relatively new interest in the generation of photonic two-frequency superposition states as qubits [12,13], the all-optical SG effect might serve as a new platform for such manipulations of light, both in the classical and the quantum domains.

In the original SG experiment [1], a beam of silver atoms, each carrying a net spin-1/2, is incident upon a region in space with a spatially varying magnetic field. We denote the propagation direction as $\hat{\mathbf{z}}$, and the transverse directions as $\hat{\mathbf{x}}$ and $\hat{\mathbf{y}}$, as illustrated in Fig. 1(a). The beam deflection due to the magnetic field gradient is later observed on a screen. Only two discrete deflection angles are observed, indicating that each of the spin components *always* has only two available values, $\pm\hbar/2$.

We shall now present the formalism reproducing the famous SG results in an analogous, classical nonlinear optical system. It is known that the linear paraxial Helmholtz equation is equivalent to the Schrödinger equation [14–16]. Furthermore, the equivalence between

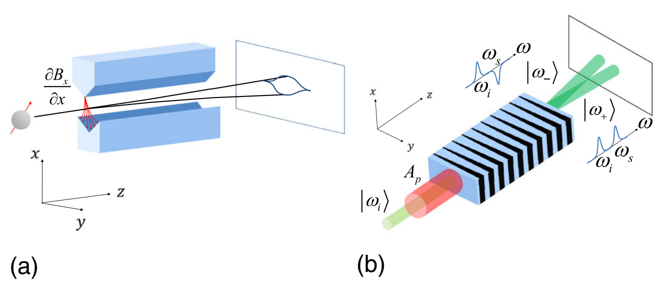


FIG. 1. (a) Setup of the original SG experiment. A beam of spin-1/2 silver atoms is deflected into two discrete directions due to a magnetic field gradient. (b) Setup of the all-optical SG experiment. An idler beam is incident on a pumped nonlinear $\chi^{(2)}$ crystal, and is deflected into two mutual beams, each composed of a superposition of the idler and signal waves. This deflection into two discrete directions occurs due to a transverse gradient in the nonlinear coupling.

 

the SFG CWEs and two-level systems has been pointed out, giving rise to the realization of robust, broadband, and efficient adiabatic frequency conversion [17–20]. Here we utilize these analogies one step further and introduce a new state of classical light, analogous to a spin-1/2 particle, and study its dynamics in the equivalent of a spatially varying magnetic field.

The time-independent, paraxial CWEs for SFG under the approximations of slowly varying envelope and undepleted pump field are given by [21]

$$\nabla_T^2 A_i + 2ik_i \frac{\partial A_i}{\partial z} = -\frac{4d\omega_i^2}{c^2} A_p^* A_s e^{-i\Delta kz}, \quad (1)$$

$$\nabla_T^2 A_s + 2ik_s \frac{\partial A_s}{\partial z} = -\frac{4d\omega_s^2}{c^2} A_p A_i e^{i\Delta kz}, \quad (2)$$

where $A_j(\mathbf{r})$ with $j = i,\ p,\ s$ (for idler, pump, and signal, respectively) are the slowly varying envelopes of the interacting waves, $k_j \simeq k_{z,j}$ and $\omega_j$ are the wave numbers and frequencies, respectively, where we set $\omega_s = \omega_i + \omega_p$, $d$ is the corresponding component of the nonlinear susceptibility tensor, $c$ the speed of light, and $\Delta k = k_p + k_i - k_s$ is the phase mismatch parameter. The nonlinear susceptibility is often modulated, a process known as quasi-phase-matching (QPM) [21,22]. In such a case, we can write the nonlinear coefficient as a Fourier series, $d(z) = \sum_q d_q e^{iqz}$, and by substituting into Eqs. (1) and (2), we keep in the rhs only the terms which oscillate closest to phase matching, similarly to the rotating wave approximation. Furthermore, we make a transformation to a rotating frame given by $A_i = \sqrt{k_s}\omega_i e^{-i(\Delta k-q)z/2}\tilde{A}_i$ and $A_s = \sqrt{k_i}\omega_s e^{i(\Delta k-q)z/2}\tilde{A}_s$, denote $A_p = |A_p|e^{i\phi_p}$ and $d_q = |d_q|e^{i\phi_d}$, and introduce dimensionless spatial coordinates $(\tilde{x}, \tilde{y}, \tau) = \sqrt{k_i k_s}(x, y, z)$.

Our goal is to demonstrate the similarity between the nonlinear coupled wave equations and the dynamics of a massive spin-1/2 particle in a magnetic field. We therefore define the square root of the ratios between the signal and idler wave vectors as spin-dependent masses, given by $m_\uparrow = \sqrt{k_i/k_s}$ and $m_\downarrow = \sqrt{k_s/k_i}$, write $m \equiv 2(m_\uparrow^{-1} + m_\downarrow^{-1})^{-1} = 2\sqrt{k_i k_s}/(k_i + k_s)$ as the equivalent of twice the reduced mass, and define $\epsilon = (m_\downarrow - m_\uparrow)/(m_\downarrow + m_\uparrow) = (k_s - k_i)/(k_s + k_i)$ as the equivalent mass contrast parameter. $m_\uparrow$, $m_\downarrow$ are the mass eigenvalues of the mass operator $M$. Its inverse is given by $M^{-1} = 1/m(\mathbf{1} + \epsilon\sigma_z)$, where $\mathbf{1}$ stands for the identity operator and $\sigma_z$ is the third Pauli matrix. We can now use these definitions to rewrite the CWEs as a single matrix equation,

$$i\frac{\partial}{\partial\tau}\begin{pmatrix}\tilde{A}_i\\ \tilde{A}_s\end{pmatrix} = \left(\frac{1}{2}M^{-1}\tilde{\mathbf{p}}_T^2 - \sigma\cdot\mathbf{B}\right)\begin{pmatrix}\tilde{A}_i\\ \tilde{A}_s\end{pmatrix}, \quad (3)$$

where $\sigma = (\sigma_x, \sigma_y, \sigma_z)$ is the Pauli matrix vector [2], and $\tilde{\mathbf{p}}_T^2 = -\nabla_T^2 = -\partial_{\tilde{x}}^2 - \partial_{\tilde{y}}^2$. Here the optical equivalent of the magnetic field is given by

$$\mathbf{B} = \frac{2|d_q A_p|}{n_i n_s}(\hat{x}\cos\phi + \hat{y}\sin\phi) + \hat{z}\frac{\Delta k - q}{2\sqrt{k_i k_s}}, \quad (4)$$

where $n_j = n(\omega_j)$ is the frequency-dependent refractive index of the medium, satisfying $k_j = n_j\omega_j/c$ for $j = i,\ s$, and $\phi = \phi_p - \phi_d$ is the relative phase between the pump envelope and the modulation of the nonlinear susceptibility (phases are measured with respect to $\tau = 0$, where the total phase of the pump field is assumed to vanish). As evident from Eq. (4), the $z$ component of this field is proportional to the phase mismatch $\Delta k - q$; its transverse component's magnitude is proportional to the nonlinear coupling strength, and the direction of this component is determined by the phase $\phi$.

A new classical state of light can be deduced from the above formalism. A mutual beam of the idler and signal waves in the paraxial approximation can be described as a tensor product of the spectral amplitude of the beam with its corresponding transverse wave front. Adopting the state ket notation, we write this two-component state as $|\psi\rangle = |\omega_i\rangle \otimes \int d^2\tilde{r}\tilde{A}_i(\tilde{\mathbf{r}})|\tilde{\mathbf{r}}\rangle + |\omega_s\rangle \otimes \int d^2\tilde{r}\tilde{A}_s(\tilde{\mathbf{r}})|\tilde{\mathbf{r}}\rangle$, where $\tilde{\mathbf{r}} = \tilde{x}\hat{x} + \tilde{y}\hat{y}$ is a transverse position vector, and $|\tilde{\mathbf{r}}\rangle$ is a continuous base ket of the position representation. Different frequency kets $|\omega_j\rangle$ are orthogonal in the sense that they cannot produce an observable interference intensity pattern, and they are also distinguishable by means of spectral filtering. Explicitly, we can write $\langle\omega_j|\omega_k\rangle = \int d\omega' S_j^*(\omega')S_k(\omega') = \delta_{jk}$, where $S_j(\omega') \equiv \langle\omega'|\omega_j\rangle$ is the normalized $[\int d\omega'|S(\omega')|^2 = 1]$ spectral amplitude of the $|\omega_j\rangle$ wave, at frequency $\omega'$.

The state $|\psi\rangle$ is equivalent to a two-component spinor representing the quantum state of a nonrelativistic spin-1/2 particle. We proceed to identify the ket states $|\omega_i\rangle$ and $|\omega_s\rangle$ as the equivalents of the spin-up $|\uparrow_z\rangle$ and spin-down $|\downarrow_z\rangle$ in the $z$ basis, respectively. Only when a transverse magnetic field equivalent, or nonlinear coupling, is present, can the two "spin" states interact and mix. In the latter case, if diffraction is neglected, all the possible states of the systems can be mapped onto a Bloch sphere, with the spin-up (idler wave) and spin-down (signal wave) states located at the north and south poles of the sphere, respectively. The magnetic field then acts as a torque vector, and the system's state precesses around it [17,19]. For more details, see the Supplemental Material [23].

In what follows, we shall restrict ourselves to the following simplifying assumptions: (i) we introduce the long-wavelength pump approximation, in which $k_p \ll k_s, k_i$ such that $\epsilon \ll 1$; (ii) we assume a constant phase $\phi = \phi_0$ in all space; (iii) we assume a quasi-phase-matched interaction, i.e., $\Delta k = q$ for the SFG process (other processes such as second harmonic generation are assumed to remain mismatched, so as to not interfere with the interaction). In terms of Eq. (4), this also means that the magnetic field is transverse, i.e., $B_z = 0$, such that $\mathbf{B} \equiv \mathbf{B}_T = B\hat{\mathbf{B}}_T(\phi_0)$, where $B(\tilde{\mathbf{r}}) = 2|d_q A_p|/n_i n_s$ is the spatially

TABLE I. Summary of the physical parameters of the spin-1/2 dynamics and the equivalent system in nonlinear optics.

| Parameter | Spin-1/2 | SFG equivalent |
|---|---|---|
| Spin ($z$ basis) | $\lvert\uparrow_z\rangle$, $\lvert\downarrow_z\rangle$ | $\lvert\omega_i\rangle$, $\lvert\omega_s\rangle$ |
| Wave functions | $\psi_\uparrow$, $\psi_\downarrow$ | $\tilde{A}_i$, $\tilde{A}_s$ |
| Magnetic field | $\mathbf{B}$ | $(2\lvert d_q A_p\rvert/n_i n_s)\hat{\mathbf{B}}_T(\phi)$ $+(\Delta k - q)/2\sqrt{k_i k_s}\hat{z}$ |
| Space and time | $(x, y, t)$ | $(\tilde{x}, \tilde{y}, \tau) = \sqrt{k_i k_s}(x, y, z)$ |
| Mass | $m$ | $m_\uparrow = \sqrt{k_i/k_s} = m_\downarrow^{-1}$ |
| Magnetic moment | $\mu = e\hbar/2m$ | $\mu = 1$ |
| Transverse spin | $(\lvert\uparrow_z\rangle \pm e^{i\phi}\lvert\downarrow_z\rangle)/\sqrt{2}$ | $\lvert\omega_\pm\rangle = (\lvert\omega_i\rangle \pm e^{i\phi}\lvert\omega_s\rangle)/\sqrt{2}$ |

varying magnetic field magnitude and $\hat{\mathbf{B}}_T(\phi_0) = \hat{x}\cos\phi_0 + \hat{y}\sin\phi_0$ is its direction [24]. The above assumptions lead to an equation equivalent to the transverse Pauli equation, describing the dynamics of a nonrelativistic spin-1/2 particle in a weak transverse magnetic field, in the particle rest frame (see the Supplemental Material for details [23]),

$$i\frac{\partial}{\partial\tau}|\psi\rangle = \left(\frac{\tilde{\mathbf{p}}_T^2}{2m} - \sigma\cdot\mathbf{B}_T(\tilde{\mathbf{r}})\right)|\psi\rangle. \tag{5}$$

A summary of our formalism is given in Table I.

A scheme for realizing an all-optical SG experiment is shown in Fig. 1(b). The equivalent of a magnetic field gradient in nonlinear optics may in principle be realized either by a linearly varying pump wave front field or via a gradient in the nonlinear coefficient. Since in our analysis we assume a uniform, plane-wave pump field, we limit the discussion to the latter option (effects of a wide Gaussian pump wavefront have shown little difference in the simulations presented in the Supplemental Material [23]). An effective gradient in the $\chi^{(2)}$ nonlinearity can be implemented by a specific choice of patterning of the nonlinear crystal. Altering the sign of $d$ by using electric field poling phase matches the interaction, whereas the duty cycle of the poling determines the strength of the interaction [21,22,25]. We comment that 2D patterns have been utilized in the past in order to spatially shape and deflect frequency-converted beams [25–29].

The magnitude of the Fourier coefficient of first-order QPM with periodically modulated nonlinearity is given by [21] $d_q = (2/\pi)d\sin[\pi D(\tilde{y})]$, where $D(\tilde{y})$ is the transversely varying duty cycle. A choice of $D(\tilde{y}) = \arcsin[(\tilde{y} + \tilde{L}_y/2)/\tilde{L}_y]/\pi$, where $\tilde{L}_y$ is the transverse width of the crystal ($-\tilde{L}_y/2 \le \tilde{y} \le \tilde{L}_y/2$), yields a magnetic field equivalent of

$$\mathbf{B}_T = \hat{\mathbf{B}}_T(\phi_0)\left(\frac{1}{2}B_0 + B'\tilde{y}\right), \tag{6}$$

where $B_0 = 2d_{\mathrm{eff}}|A_p|/n_i n_s$, with $d_{\mathrm{eff}} = 2d/\pi$ and where $B' = B_0/\tilde{L}_y$ is the equivalent of a magnetic field gradient.

We now turn to solve the wave equation, Eq. (5). First, we note that a transformation from the $z$-component basis of the spin to the spin basis in the direction $\hat{\mathbf{B}}_T(\phi_0) = \hat{x}\cos\phi_0 + \hat{y}\sin\phi_0$ diagonalizes Eq. (5). This transformation is given explicitly by

$$|\omega_+\rangle = \frac{|\omega_i\rangle + e^{i\phi_0}|\omega_s\rangle}{\sqrt{2}}, \qquad |\omega_-\rangle = \frac{|\omega_i\rangle - e^{i\phi_0}|\omega_s\rangle}{\sqrt{2}}, \tag{7}$$

and we can interpret each of these eigenstates as a mutual beam of the idler and signal waves, in contrast to the previously discussed spin eigenstates along the $z$ axis, which are characterized by only a single frequency (either $\omega_s$ or $\omega_i$). Next, we transform the resulting diagonalized equation to the transverse Fourier space by taking $a_j(\tilde{\mathbf{k}}_T) = \int d^2\tilde{r}A_j\exp(-i\tilde{\mathbf{k}}_T\cdot\tilde{\mathbf{r}})$, where $\tilde{\mathbf{k}}_T = (\tilde{k}_x, \tilde{k}_y)$ is a dimensionless transverse $k$-vector, and a general state may now be written as $|\psi\rangle = \sum_{s=\omega_\pm}|s\rangle\otimes\int d^2\tilde{k}a_s(\tilde{\mathbf{k}}_T)|\tilde{\mathbf{k}}_T\rangle$. The resulting Hamiltonian in the diagonalized momentum representation is $H = H_+|\omega_+\rangle\langle\omega_+| + H_-|\omega_-\rangle\langle\omega_-|$, where $H_\pm = \frac{1}{2}\tilde{k}_T^2 \mp iB'(\partial/\partial\tilde{k}_y) \mp \frac{1}{2}B_0$. The general solution to the wave equation is given in terms of the propagation operators in the momentum representation, $U_\pm(\tau) = \int d^2\tilde{k}\exp(-i\tau H_\pm)|\tilde{\mathbf{k}}_T\rangle\langle\tilde{\mathbf{k}}_T|$. Employing the Zassenhaus formula [30], these propagation operators are found to be

$$\begin{aligned}\exp(-i\tau H_\pm) = \exp\left(\pm i\tau\frac{B_0}{2} - i\frac{\tau^3 B'^2}{6}\right)\\ \times\exp\left(\mp\tau B'\frac{\partial}{\partial\tilde{k}_y}\right)\\ \times\exp\left(-i\tau\frac{1}{2}\tilde{k}_T^2 \mp \frac{1}{2}i\tau^2 B'\tilde{k}_y\right).\end{aligned} \tag{8}$$

The structure of the propagation operator implies that each of the eigenstates [the mutual beams of Eq. (7)] accelerates in the $\pm y$ directions, with acceleration $B'$ [31]. This is the manifestation of the Stern-Gerlach dynamics in the equivalent nonlinear optics system, as illustrated in Fig. 2.

We now investigate how a Gaussian beam in the idler frequency is affected by the SG Hamiltonian. This beam is equivalent to a free "particle" with a spin-up in the $z$ direction. Note that the initial beam in the idler frequency is merely the sum of the two mutual beams, Eq. (7), as the wave in the signal frequency is absent. Therefore, at $\tau = 0$ we write the state ket as $|\psi(0)\rangle = (1/\sqrt{2})(|\omega_+\rangle + |\omega_-\rangle)\otimes\int d^2\tilde{k}a_i(\tilde{\mathbf{k}}_T)|\tilde{\mathbf{k}}_T\rangle$, where $a_i(\tilde{\mathbf{k}}_T) = A_0\exp(-\tilde{k}_T^2/2\Delta\tilde{k}^2)/\sqrt{\pi\Delta k^2}$, and the state at any time $\tau$ will be given by $|\psi(\tau)\rangle = [\exp(-i\tau H_+)|\omega_+\rangle\langle\omega_+| + \exp(-i\tau H_-)|\omega_-\rangle\langle\omega_-|]|\psi(0)\rangle$. The action of each propagator on the Gaussian envelope deflects the mutual beams into two discrete directions. The Fourier space intensity of each of the spin states in terms of dimensional parameters, just outside the crystal, is therefore given by

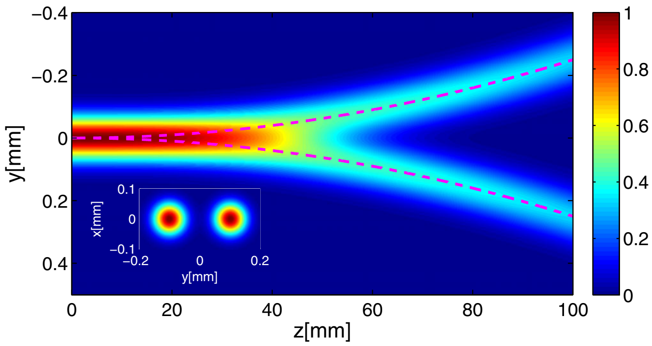


FIG. 2. Total intensity pattern (in arbitrary units) describing the propagation of a Gaussian idler beam inside a nonlinear-optical SG apparatus. The idler beam is deflected into two mutual beams, each comprising the idler and signal waves. Inside the crystal, the beams follow an accelerated trajectory (dashed lines). Inset: the far-field intensity (for $L_z = 2.3$ cm, $R = 10$ cm) with $\theta = 1$ mrad.

$$|\langle \mathbf{k}_0, \pm|\psi\rangle|^2 = \frac{|A_0|^2}{2\pi\Delta k^2}\exp\left(-\frac{k_{0,x}^2 + (k_{0,y} \mp \theta k_{0,z})^2}{\Delta k_0^2}\right), \quad (9)$$

where $\mathbf{k}_0 = (k_{0x}, k_{0y}, k_{0z})$ is the free-space wave vector. The deflection angle, $\theta$, is given by

$$\theta = n_i \tau B' = \sqrt{\frac{I_p}{I_0}\frac{L_z}{L_y}}, \quad (10)$$

where we have used $B' = 2|A_p|d_{\mathrm{eff}}/n_i^3 k_0 L_y$, and where the reference intensity is defined as $I_0 = \frac{1}{2} n_p n_i^2 \epsilon_0 c d_{\mathrm{eff}}^{-2}$. The deflection angle is the product of the time of flight of the "particle" and the magnetic field gradient, and is therefore proportional to the crystal length and inversely proportional to the crystal width. A surprising result is that there is not any on-axis light—either at the original idler frequency or at the signal frequency—despite the fact that the up-conversion process is collinearly phase matched. It is also interesting to note that the deflection angle is all-optically controlled by the pump intensity, and increases as the interaction length becomes larger. Substituting typical values for $\mathrm{LiNbO_3}$, $d_{\mathrm{eff}} = 17.2 \times 10^{-12}$ m/V, $\lambda_i = 500$ nm, $\lambda_p = 3500$ nm, $n_p = 2.14$, and $n_i = 2.34$, we find $I_0 \simeq 5.26 \times 10^{15}$ W/cm$^2$. Choosing crystal dimensions $L_y = 1$ mm and $L_z = 2.3$ cm, and for a pulsed pump of peak intensity $\sim$10 MW/cm$^2$, we find $\theta \simeq 1$ mrad.

At a distance $R$ from the nonlinear crystal, this deflection produces a far-field intensity distribution of

$$I(\mathbf{r}) \propto \frac{1}{\lambda_0^2 R^2}\sum_{s=\omega_\pm} |\langle \mathbf{k}_0, s|\psi\rangle|^2 \left(\frac{k_0 \mathbf{r}}{R}\right), \quad (11)$$

where $\mathbf{r} = \hat{\mathbf{x}}x + \hat{\mathbf{y}}y$ is the position on the screen, and $|\langle \mathbf{k}_0, s|\psi\rangle|^2$ is given in Eq. (9). The inset in Fig. 2 illustrates the intensity pattern in the far field. This intensity pattern has two distinct lobes, as in the SG experiment. We emphasize that each of the spots on the screen contains a similar contribution from both the idler and signal waves, having a phase difference of $\phi_0$ (for the $|\omega_+\rangle$ state) or $\phi_0 + \pi$ (for the $|\omega_-\rangle$ state). A numerical simulation corresponding to our analytic derivations is presented in the Supplemental Material [23].

In summary, we have introduced a novel formalism in which a mutual beam of light undergoing a nonlinear interaction is equivalent to a spin-1/2 particle in a spatially varying magnetic field. We presented the possibility of an all-optical Stern-Gerlach effect, where an idler beam is deflected by a gradient in the nonlinear coupling, into two mutual beams propagating in two discrete directions. Our formalism may certainly lead to other interesting analogies to physical effects of spin-1/2 dynamics. For example, an adiabatic Berry phase can be realized in nonlinear optics [32], where the mutual beam is expected to accumulate a $\pi$ phase shift upon a $2\pi$ rotation of the state, as do spin-1/2 particles and polarized photons following a rotation over a great circle on the Bloch and Poincaré spheres, respectively [2,33–35].

A further outlook into quantum effects can occur when the input idler wave is a single photon state. In this case, the result will be a single-photon 2-qubit state in both frequency, i.e., either the signal or the idler frequencies, as well as in direction, in one of the two output angles. This observation might be of importance for generating, and spatially separating, orthogonal frequency superposition states for the realization of bichromatic qubits [12,13]. A Stern-Gerlach deflector for single photons may, therefore, play an important role in the realization of quantum information applications based on photonic qubits in the frequency basis.

The all-optical SG effect may also provide a platform for investigating just how far can the limits of analogies between classical and quantum-mechanical systems be stretched. For example, controversial concepts such as classical or single-particle "entanglement" [36–38] can be put to experimental investigation. This may cast light on the quantum mechanical phenomena and the mechanisms that suppress them in the classical description of the macroscopic world.

This work was supported by the Israel Science Foundation, Grant No. 1415/17.

[1] W. Gerlach and O. Stern, Der experimentelle Nachweiss der Richtungsquantelung im Magnetfeld, Z. Phys. 9, 349 (1922).
[2] J. J. Sakurai and J. Napolitano, *Modern Quantum Mechanics*, 2nd ed. (Addison-Wesley, San Francisco, 2011).
[3] D. Griffiths, *Introduction to Quantum Mechanics*, 2nd ed. (Pearson Education, Upper Saddle River, NJ, 2005).

[4] R. J. Cook, Optical Stern-Gerlach effect, Phys. Rev. A **35**, 3844 (1987).
[5] E. Gershnabel, M. Shapiro, and I. Sh. Averbukh, Stern-Gerlach deflection of field-free aligned paramagnetic molecules, J. Chem. Phys. **135**, 194310 (2011).
[6] H. Dehmelt, Continuous Stern-Gerlach effect: Principle and idealized apparatus, Proc. Natl. Acad. Sci. U.S.A. **83**, 2291 (1986).
[7] C. H. Chern, C. J. Lin, and C. T. Liang, Proposed Non-magnetic Stern-Gerlach Experiment Using Electron Diffraction, Phys. Rev. Lett. **105**, 217205 (2010).
[8] L. Kapra and M. Weitz, A Stern-Gerlach experiment for slow light, Nat. Phys. **2**, 332 (2006).
[9] C. Hang and G. Huang, Stern-Gerlach effect of weak-light ultraslow vector solitons, Phys. Rev. A **86**, 043809 (2012).
[10] Y. Guo, L. Zhou, L. M. Kuang, and C. P. Sun, Magneto-optical Stern-Gerlach effect in an atomic ensemble, Phys. Rev. A **78**, 013833 (2008).
[11] G. I. Stegeman, D. J. Hagan, and L. Torner, $\chi^{(2)}$ cascading phenomena and their applications to all-optical signal processing, mode-locking, pulse compression and solitons, Opt. Quantum Electron. **28**, 1691 (1996).
[12] S. Clemmen, A. Farsi, S. Ramelow, and A. L. Gaeta, Ramsey Interference with Single Photons, Phys. Rev. Lett. **117**, 223601 (2016).
[13] P. Treutlein, Viewpoint: Photon qubit is made of two colors, Physics **9**, 135 (2016).
[14] M. A. M. Marte and S. Stenholm, Paraxial light and atom optics: The optical Schrödinger equation and beyond, Phys. Rev. A **56**, 2940 (1997).
[15] O. Steuernagel, Equivalence between focused paraxial beams and the quantum harmonic oscillator, Am. J. Phys. **73**, 625 (2005).
[16] G. A. Siviloglou and D. N. Christodoulides, Accelerating finite energy Airy beams, Opt. Lett. **32**, 979 (2007).
[17] H. Suchowski, D. Oron, A. Arie, and Y. Silberberg, Geometrical representation of sum frequency generation and adiabatic frequency conversion, Phys. Rev. A **78**, 063821 (2008).
[18] H. Suchowski, G. Porat, A. Arie, and Y. Silberberg, Adiabatic processes in frequency conversion, Laser Photonics Rev. **8**, 333 (2014).
[19] H. Suchowski, V. Prabhudesai, D. Oron, A. Arie, and Y. Silberberg, Robust adiabatic sum frequency conversion, Opt. Express **17**, 12731 (2009).
[20] P. Krogen, H. Suchowski, H. Liang, H. Flemens, K. H. Hong, F. X. Kartner, and J. Moses, Generation and multi-octave shaping of mid-infrared intense single-cycle pulses, Nat. Photonics **11**, 222 (2017).
[21] R. W. Boyd, *Nonlinear Optics*, 3rd ed. (Academic Press, New York, 2008).
[22] A. Arie and N. Voloch, Periodic, quasi-periodic, and random quadratic nonlinear photonic crystals, Laser Photonics Rev. **4**, 355 (2010).
[23] See Supplemental Material at http://link.aps.org/supplemental/10.1103/PhysRevLett.120.053901 for the derivations of the transverse Pauli equation, the mapping of SFG to the Bloch sphere and the SG propagator, as well as for numerical simulations of the effect.
[24] The magnetic field analogue need not have a vanishing divergence, i.e., $\nabla \cdot \mathbf{B}_T \neq 0$ in general.
[25] M. Yamada, N. Nada, M. Saitoh, and K. Watanabe, First-order quasi-phase matched LiNbO3 waveguide periodically poled by applying an external field for efficient blue second-harmonic generation, Appl. Phys. Lett. **62**, 435 (1993).
[26] M. Yamada and M. S. Ooki, Electric-field induced cylindrical lens, switching and deflection devices composed of the inverted domains in LiNbO3 crystals, Appl. Phys. Lett. **69**, 3659 (1996).
[27] T. Ellenbogen, A. Ganany-Padowicz, and A. Arie, Nonlinear photonic structures for all-optical deflection, Opt. Express **16**, 3077 (2008).
[28] A. Shapira, L. Naor, and A. Arie, Nonlinear optical holograms for spatial and spectral shaping of light waves, Science bulletin **60**, 1403 (2015).
[29] S. Trajtenberg-Mills, I. Juwiler, and A. Arie, Generation of second-harmonic beams with switchable curved trajectories, Optica **4**, 153 (2017).
[30] F. Casas, A. Murua, and M. Nadinic, Efficient computation of the Zassenhaus formula, Comput. Phys. Commun. **183**, 2386 (2012).
[31] This property is reminiscent of the well-known Airy beams which exhibit such acceleration. It is of no coincidence, since the Airy functions arise as the eigenfunctions of the SG Hamiltonian in the position representation.
[32] A. Karnieli and A. Arie, Fully controllable adiabatic geometric phase in nonlinear optics, Opt. Express (to be published).
[33] R. Y. Chiao and Y. S. Wu, Manifestations of Berry's Topological Phase for the Photon, Phys. Rev. Lett. **57**, 933 (1986).
[34] M. V. Berry, The adiabatic phase and Pancharatnam's phase for polarized light, J. Mod. Opt. **34**, 1401 (1987).
[35] K. Wang, Y. Shi, A. S. Solntsev, S. Fan, A. A. Sukhorukov, and D. N. Neshev, Non-reciprocal geometric phase in nonlinear frequency conversion, Opt. Lett. **42**, 1990 (2017).
[36] G. B. Roston, M. Casas, A. Plastino, and A. R. Plastino, Quantum entanglement, spin-1/2 and the Stern-Gerlach experiment, Eur. J. Phys. **26**, 657 (2005).
[37] R. J. C. Spreeuw, A classical analogy of entanglement, Found. Phys. **28**, 361 (1998).
[38] E. Karimi and R. W. Boyd, Classical entanglement?, Science **350**, 1172 (2015).